J Polym Res (2015) 22: 110
DOI 10.1007/s10965-015-0758-7

ORIGINAL PAPER

Effect of living polystyrene costabilizer on styrene miniemulsion polymerization

Chun-Ta Lin[1] · **Shao-En Yu**[1] · **Chorng-Shyan Chern**[1]

Received: 19 November 2014 / Accepted: 11 May 2015 / Published online: 16 May 2015

Abstract RAFT miniemulsion polymerizations of styrene with living polystyrene (PS_{lc}) serving as both RAFT reagent and polymer costabilizer were investigated. The miniemulsion upon aging at 25 °C showed satisfactory stability against the Ostwald Ripening process. The rate of polymerization for RAFT miniemulsion polymerization initiated by oil-soluble AIBN is much slower than that for the water-soluble SPS counterpart. In addition to the predominant monomer droplet nucleation, much stronger particle nucleation taking place in the continuous aqueous phase (homogeneous nucleation) for the run with AIBN was observed. It is the different extents of homogeneous nucleation that is responsible for the quite different kinetic behaviors between the RAFT miniemulsion polymerizations initiated by different types of initiator (AIBN versus SPS). Furthermore, increasing initial molar ratio of RAFT reagent to AIBN greatly enhances the characteristics of RAFT polymerization (i.e., better control over polymer chain growth with the progress of polymerization).

Keywords RAFT miniemulsion polymerization · Living polymer costabilizer · Ostwald ripening · Kinetics

Introduction

Controlled/living free radical polymerizations are of increasing importance in industry because they are capable of synthesizing polymeric materials with well controlled molecular weight and molecular weight distribution, molecular architecture and desirable end-functionalities [1, 2]. Some representative techniques include nitroxide-mediated polymerization (NMP) [3], atom transfer radical polymerization (ATRP) [4] and reversible addition fragmentation transfer polymerization (RAFT) [5–7]. The principles of NMP and ATRP are based on reversible termination reaction, whereas RAFT is based on reversible chain transfer reaction [8]. Among these approaches, perhaps RAFT polymerization is the most promising one because it offers many advantages such as compatible with a wide range of monomers, a broad range of reaction conditions and a variety of processes (e.g., bulk, suspension, emulsion and miniemulsion) [9–12].

The key feature of RAFT polymerization is the chain equilibrium reaction between propagating radicals and dormant species, as shown in Scheme 1 [13]. The activating group must activate the carbon-carbon double bond of monomer toward radical addition, but not imparts significant stabilization to intermediate radical. In contrast, the leaving group should be a good homolytic species and capable of reinitiating polymerization [14, 15]. Thiocarbonyl compounds such as dithiocarbamates, xanthates, dithiocarbonates and trithiocarbonates are commonly used as RAFT reagents [5]. Among these RAFT reagents, trithiocarbonates (e.g., dibenzyl trithiocarbonate (DBTTC) illustrated in Scheme 1) are of great importance as they contain two homolytic leaving groups that allow polymer chain segments grow in two directions. In addition, trithiocarbonates exhibit high chain transfer constant and are hydrolytically stable [16, 17].

Emulsion polymerization is an important process widely used in plant production of water-based polymers for industrial applications such as thermoplastics, paints and coatings and adhesives because it provides a green process in large scale production, easy heat removal and convenient handling

✉ Chorng-Shyan Chern
cschern@mail.ntust.edu.tw

[1] Department of Chemical Engineering, National Taiwan University of Science and Technology, Taipei 106, Taiwan

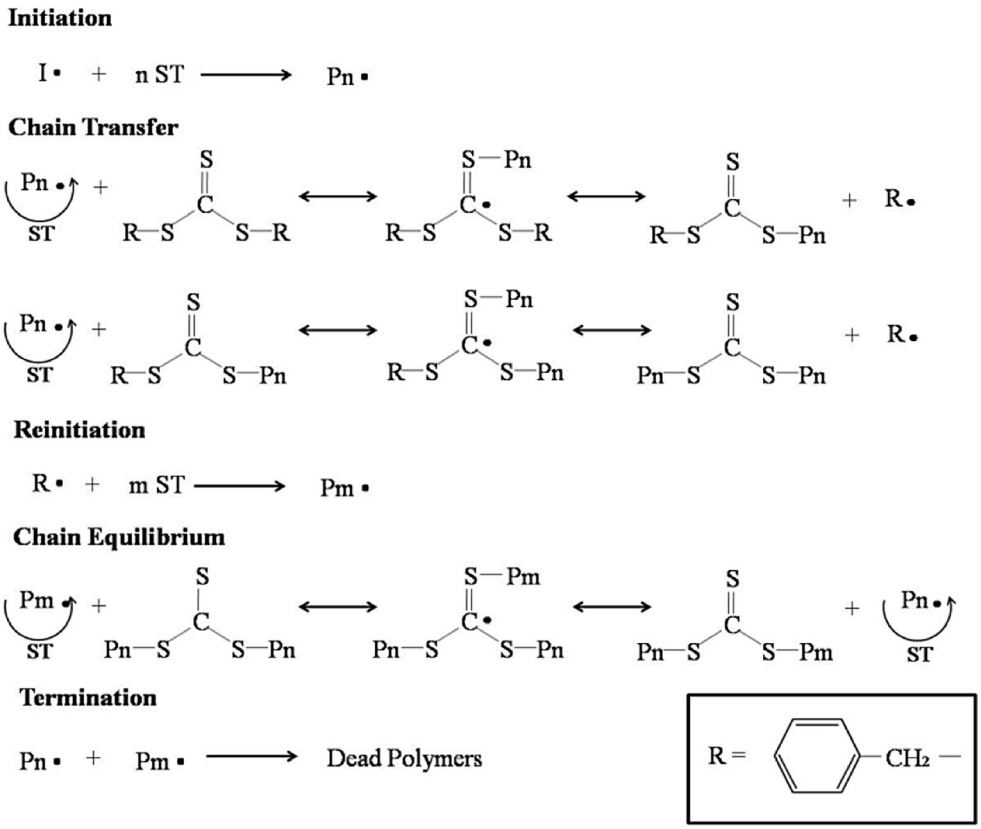

Scheme 1 The mechanism of RAFT polymerization of ST using dibenzyl trithiocarbonate (DBTTC) as RAFT reagent, where I is the initiator radical, P_m and P_n are the polymeric radicals with m and n units of styrene (ST), respectively, and R is the radical originating from the leaving group. Note that R serves as both activating and leaving groups in RAFT polymerization

of final products with high solids content [18, 19]. However some problems such as poor control in polymer molecular weight and molecular weight distribution, transport of very hydrophobic species in heterogeneous reaction system, high level of coagulum and phase separation occur during polymerization [20–23]. Living RAFT miniemulsion polymerization serves as an alternative to overcome these problems. Miniemulsion is prepared by homogenizing a mixture of monomer, water, surfactant and costabilizer under high shearing to achieve submicron monomer droplet size (50–500 nm in diameter) [24, 25]. The resultant miniemulsion droplets exhibit an extremely large total oil–water interfacial area available for particle nucleation therein. The extremely hydrophobic costabilizer incorporated into miniemulsion droplets suppresses diffusion of monomer from small droplets with higher interfacial energy to large droplets with lower interfacial energy (termed Ostwald Ripening). Incorporation of surfactant into the colloidal system is a must in order to prevent coalescence among miniemulsion droplets and achieve high colloidal stability. Anionic surfactants are commonly used to provide adequate miniemulsion stability during storage and polymerization [26–28]. Reimers and Schork [29, 30], employed polymethyl methacrylate as costabilzer in stabilizing miniemulsions against Ostwald ripening and then studied particle nucleation mechanisms involved in subsequent miniemulsion polymerizations. They claimed that it was the monomer droplet nucleation that predominated in the polymerization.

In this study, the authors synthesized living polystyrene using DBTTC as RAFT reagent and then used it as costabilizer (denoted as PS_{lc}) in ST miniemulsion polymerizations. The objective of this work was to evaluate the effectiveness of PSlc in stabilizing ST miniemulsions against diffusional degradation of submicron monomer droplets upon aging at room temperature. Another major thrust was to investigate the mechanisms and kinetics involved in RAFT miniemulsion polymerizations of ST with PSlc acting as both RAFT reagent and costabilizer. The results obtained from this work may help gain a better understanding of RAFT polymerization occurring within a large population of submicron reactors (i.e., miniemulsion droplets).

Experimental

Materials

The chemicals used include styrene (ST, Taiwan Styrene), sodium dodecylbenzene sulfonate (SDBS, Sigma-Aldrich), Emulgen 950 (a polyoxyethylene nonylphenyl ether with 50 units of ethylene oxide, Kao Soap), sodium bicarbonate

(Riedel de Haen), sodium persulfate (SPS, Riedel de Haen), 2, 2′-azobisisobutyronitrile (AIBN, Sigma-Aldrich), benzyl chloride (Acros), carbon disulfide (Panreac), sodium sulfide hydrate (Acros), tributylmethylammonium chloride solution (75 %, Acros), methanol (Union Chemical Ind.), ethanol (Union Chemical Ind.), a series of polystyrene (PS) standards for gel permeation chromatography (GPC) calibration (Shodex), tetrahydrofuran (THF, Acros), nitrogen (Ching-Feng-Harng) and deionized water (Barnsted, Nanopure Ultrapure Water System, specific conductance <0.057 μS cm^{-1}). ST was purified at 40 °C under reduced pressure and stored at 4 °C before use. Other chemicals were reagent grade and used as received.

Preparation and characterization of living polystyrene costabilizer

DBTTC was synthesized according to the literature [31]. First, 58.5 g of sodium sulfide hydrate, 3 g of 75 % aqueous solution of tributylmethylammonium chloride, 35.4 g of carbon disulfide and 150 mL water were charged to a 500-mL reactor equipped with a mechanical agitator and a thermometer. The mixture was then stirred for 1 h. The reaction mixture turned to bright red immediately after sodium trithiocarbonate was produced. Subsequently, 100.8 g of benzyl chloride was added to the reactor over a period of 15 min. The mixture was stirred at 50 °C for 3 h and then at 70 °C for additional 30 min. To complete the reaction, 1.5 g of tributylmethylammonium chloride was added to the reaction mixture without heating overnight. A yellow semi-solid product containing DBTTC (bottom layer) was separated from the aqueous phase (upper layer) using a funnel separator. The crude DBTTC product was washed repeatedly by excessive ethanol. The crystalline product was then filtered and dried at 50 °C. The product was characterized by ^{1}H-NMR and ^{13}C-NMR.

Living polystyrene costabilizer (PS_{lc}) was prepared by an isothermal bulk RAFT polymerization process. First, 50 g of ST and 1.39 g of DBTTC (RAFT reagent) were charged to a 100-mL reactor equipped with a mechanical agitator, a reflux condenser and a thermometer immersed in a thermostatic oil bath. The reaction mixture was then purged by nitrogen for 10 min to remove dissolved oxygen, followed by raising the reactor temperature to 110 °C. The thermal polymerization of ST in the presence of DBTTC then proceeded for 24 h. The resultant PS_{lc} was precipitated by excessive methanol and allowed to stand overnight. This was followed by filtration and then thorough rinse of PS_{lc} by excessive methanol and water. The PS_{lc} sample thus collected was dried in a vacuum oven at 60 °C over a period of 24 h. The number-average molecular weight (M_n) and polydispersity index (PDI=M_w/M_n, where M_w is the weight-average molecular weight) data for PS_{lc} were determined by GPC (Waters, 2410) in combination with a calibration curve established by a series of PS standards.

Preparation and characterization of miniemulsions

ST miniemulsion was prepared by dissolving 8 mM of SDBS, 0.6 mM of Emulgen 950 and 2.66 mM of sodium bicarbonate in 114 g of water and dissolving 2.77 g of PS_{lc} in 27.23 g of ST, respectively. The volume fraction of PS_{lc} in ST (φ_p) was 0.08. This was followed by mixing the oily and aqueous solutions with a mechanical agitator at 500 rpm for 10 min. The resultant emulsion was then homogenized with the ultrasonic homogenizer (Misonic sonicator 3000) for 24 cycles of 100 s in length with 40 s off-time, and the output power was set at 24 W. The hydrodynamic miniemulsion droplet diameter (d_m) data were obtained from dynamic light scattering (DLS, Malvern, Zetasizer 1000HS_A). The sample was diluted with water to eliminate the multiple scattering effect. The dilution water was saturated with SDBS (critical micelle concentration (CMC)=1.8 mM [32]), Emulgen 950 (CMC=0.294 mM [33]) and ST. In this manner, diffusion of SDBS, Emulgen 950 and ST species from miniemulsion droplets into the continuous aqueous phase was prohibited.

ST miniemulsion polymerization kinetics

Immediately after homogenization, the resultant miniemulsion was charged into a 500-mL reactor equipped with a four-bladed fan turbine agitator, a thermocouple and a reflux condenser and then purged with nitrogen for 10 min to remove dissolved oxygen, while the reactor temperature was brought to 70 °C. The initiator solution (2.8 mM of water-soluble SPS based on total water volume) was then charged into the reactor to start the polymerization, and the temperature was kept constant at 70 °C throughout the reaction. For the polymerization initiated by oil-soluble AIBN, 0.08 g of AIBN was dissolved in the oil phase containing 2.77 g of PS_{lc} and 27.23 g of ST immediately before the preparation of miniemulsion. The agitation speed was set at 350 rpm over a period of 6 h. The latex product was filtered through 40-mesh and 200-mesh screens in series. The hydrodynamic particle diameter (d) of the sample taken during the reaction was determined by DLS. In addition, the morphology of final latex particles was observed by transmission electron microscopy (TEM, Jeol, JEM-1400). Fractional monomer conversion (X) was determined by the gravimetric method. Evolution of molecular weight and molecular weight distribution of polymer during the reaction was measured by GPC (Waters, 2410)

Results and discussion

Characterization of living polystyrene costabilizer

Figure 1 shows the ^{1}H-NMR spectrum of DBTTC, in which the ratio of the integral area of the characteristic peak at chemical shift (δ)=4.684 ppm (a) to that of the characteristic peak at δ=7.3–7.4 ppm (b) is 1:2.45, which is reasonably consistent with the theoretical ratio (1:2.50). The characteristic peaks of DBTTC obtained from ^{13}C-NMR spectrum further confirm the molecular structure of DBTTC (Fig. 2).

M_n and PDI of PS_{lc} obtained from GPC (Fig. 3) are 8703 g mol^{-1} and 1.09, respectively. The very narrow molecular weight distribution (PDI=1.09) reflects the major characteristics of bulk RAFT polymerization used in this work.

Ostwald ripening behavior of ST miniemulsions

Effect of polymer costabilizer molecular weight

According to Morton equation [30, 34], the chemical potential ($\triangle\mu_m$) of a two-component disperse phase system, in which droplets of monomer and polymer dispersed in the continuous aqueous phase can be expressed as follows:

$$\Delta\mu_m = \ln\left(1-\varphi_p\right)(1-1/n)\varphi_p + \chi_{mp}\varphi_p{}^2 + a/\alpha \qquad (1)$$

where φ_p is the volume fraction of polymer in the oil phase, n is the number-average degree of polymerization, χ_{mp} is the interaction parameter between monomer and polymer, a is the droplet radius, and α is defined as $2\sigma V_m/(RT)$, in which V_m is the molar volume of monomer and σ is the oil–water interfacial tension. As expected, the larger the value of n (i.e., polymer molecular weight), the higher the $\triangle\mu_m$. This implies that the effectiveness of polymer costabilizers in retarding the Ostwald ripening process involved in a two-component disperse phase system decreases with increasing polymer costabilizer molecular weight. Thus, higher levels of polymer costabilizer are generally required to produce stable ST miniemulsions, as compared to low molecular weight costabilizers such as hexadecane. However, the effect of polymer costabilizer molecular weight is beyond the scope of this work. For those who are interested in this subject, refer to our previous study [35], in which the effect of polymer costabilizer molecular weight on the Ostwald ripening rate (R_O) was confirmed. It is noteworthy that the molecular weight (8703 g mol^{-1}) of PS_{lc} is low enough to prepare kinetically stable ST miniemulsions in this study.

Ostwald ripening rate of ST miniemulsions

Figure 4 shows the d_m^3 versus time (t) data for the ST miniemulsion upon standing at 25 °C. The Ostwald ripening experiment was carried out twice to test the reproducibility.

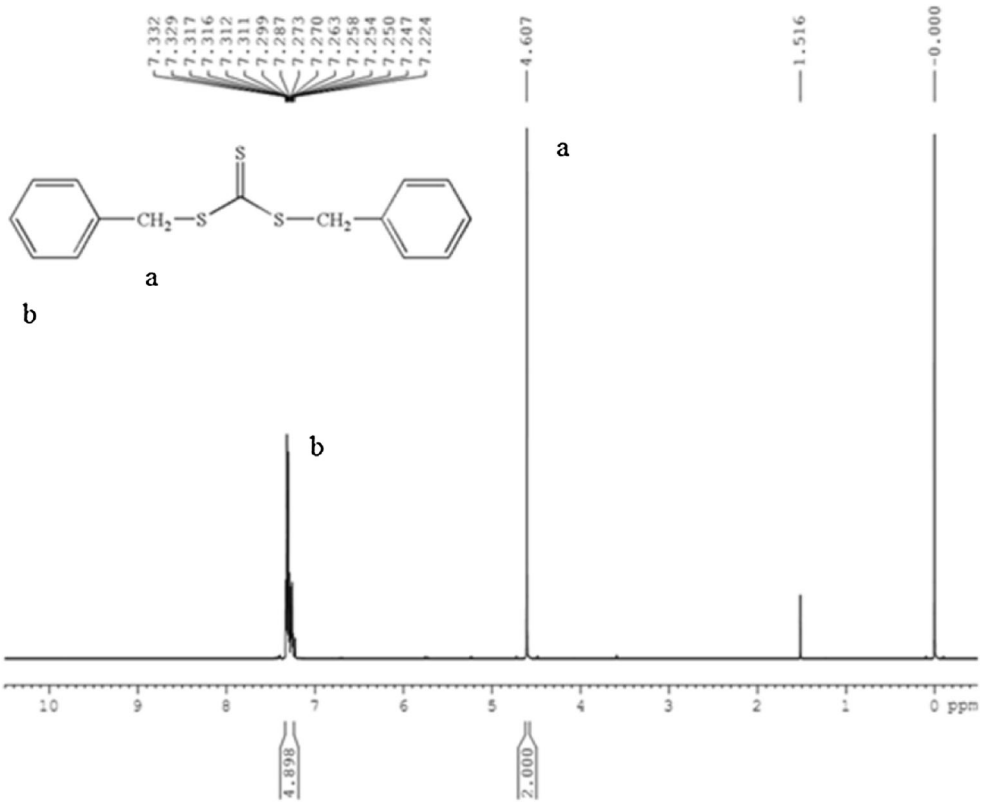

Fig. 1 ^{1}H-NMR spectrum of DBTTC

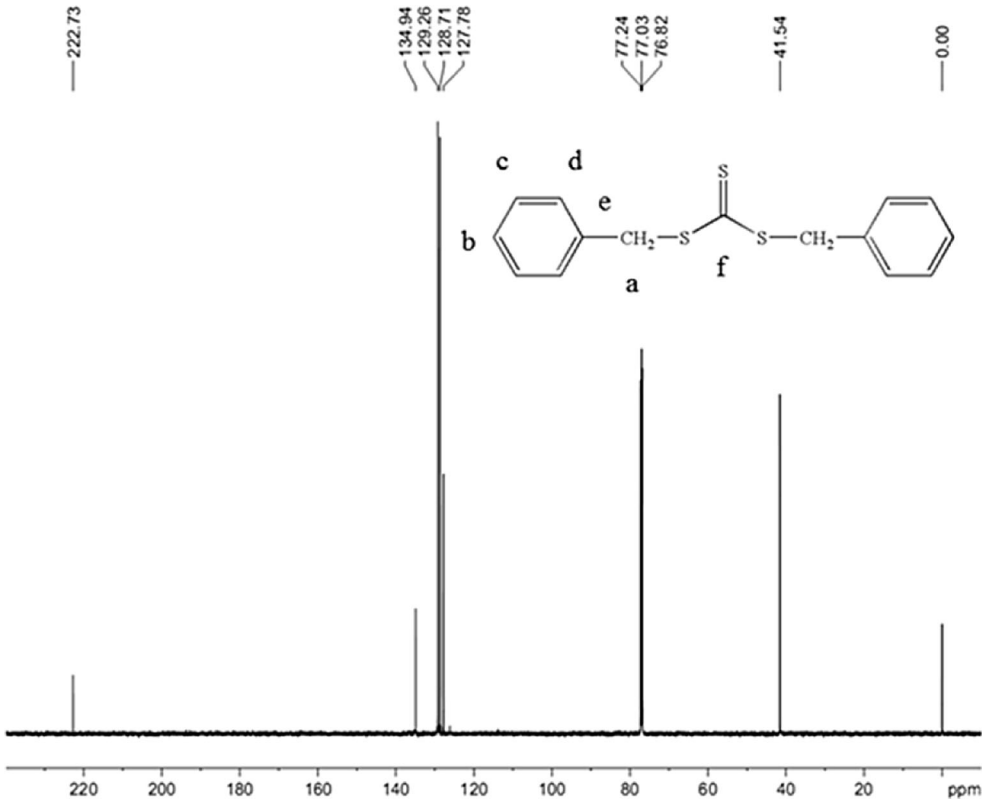

Fig. 2 ^{13}C-NMR spectrum of DBTTC

The Ostwald ripening rate (R_O=1/8 [d(d_m^3)/dt]) [36, 37] obtained from the slope of the least-squares best-fitted straight line was (5.27±1.06)×10^{-21} cm^3 s^{-1}. For comparison, some representative R_O data for ST miniemulsions stabilized by conventional polystyrene costabilizers (PS_c) with comparable M_n but much larger PDI taken from our previous studies [35] are listed in Table 1. It is interesting to note that, for ST miniemulsions with φ_p=0.08, PS_{lc} is more effective in retarding the Ostwald ripening process than PS_c. This is most likely due to the very narrow molecular weight distribution of PS_{lc} in comparison with the PS_c counterparts. In other words, a significant fraction of a particular PS_c with a relatively large PDI exhibits higher molecular weight than its M_n and, therefore, this part of PS_c species does not effectively stabilize ST miniemulsion against Ostwald ripening.

Polymerization kinetics of ST miniemulsions

The X versus t profiles for the miniemulsion polymerization of ST stabilized by PS_{lc} (φ_p=0.08) and initiated by 2.8 mM

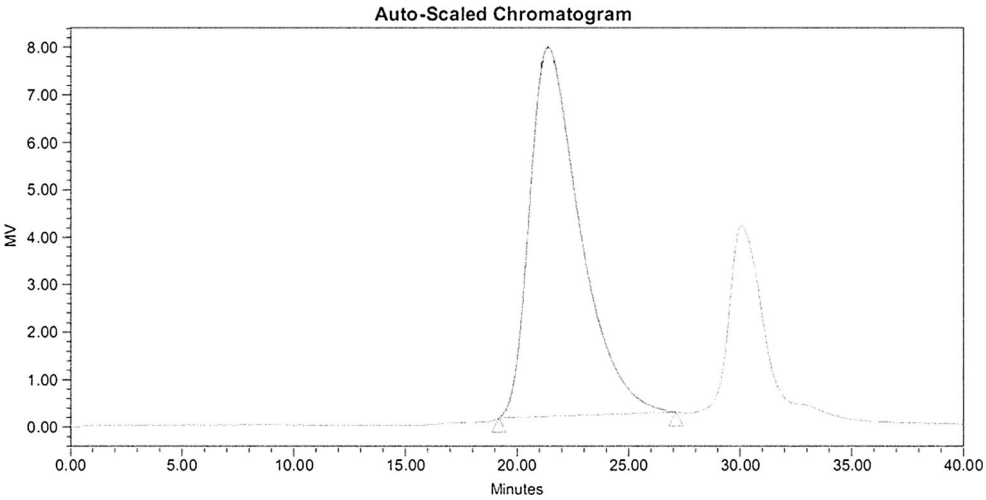

Fig. 3 GPC curve of living polystyrene costabilizer

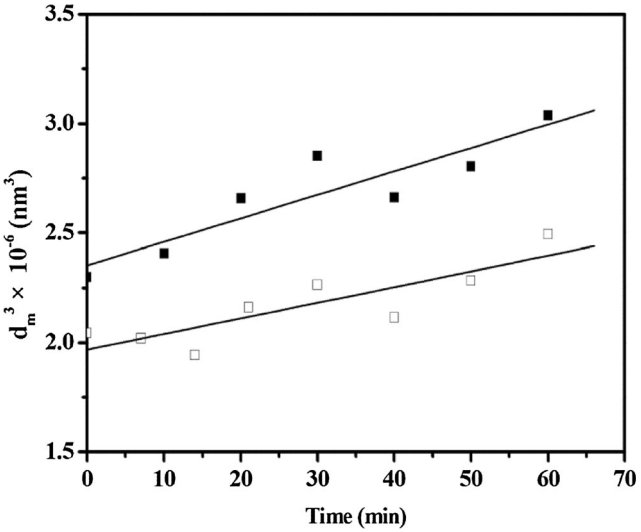

Fig. 4 Representative d_m^3 versus time data for ST miniemulsion stabilized by the living polystyrene costabilizer with M_n=8703 g mol^{-1} and φ_p=0.08. The Ostwald ripening experiment in duplicate was carried out to test the reproducibility

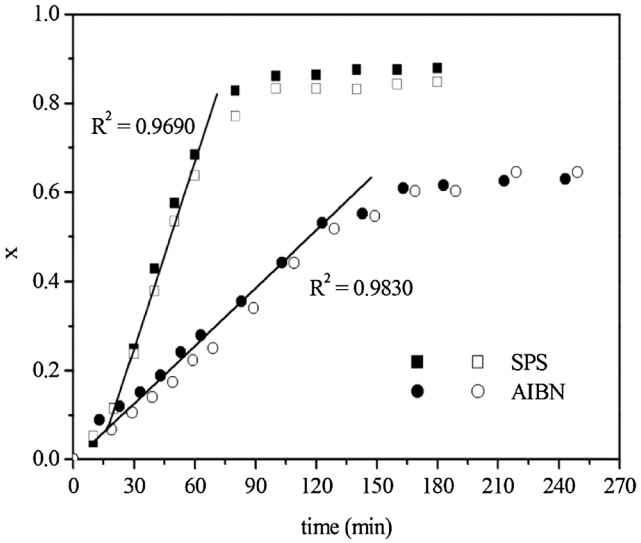

Fig. 5 Monomer conversion versus time profiles for the miniemulsion polymerization of ST stabilized by PS_{lc} (φ_p=0.08) and initiated by SPS or AIBN at 70 °C. The rate of polymerization was obtained from the slope of the least-squares best-fitted straight line passing the linear part of the X versus t data points. (*filled square*, *white square*) SPS (R^2=0.9690), (*filled circle*, *white circle*) AIBN (0.9830)

SPS based on total water volume or 15.0 mM AIBN based on the oil phase volume at 70 °C are shown in Fig. 5. Each polymerization was carried out in duplicate to evaluate the experimental reproducibility. The reproducibility of the duplicate polymerization initiated by SPS or AIBN is quite satisfactory, as shown by the open and closed data points in Fig. 5. It is shown that the rate of polymerization (R_p=6.6×10^{-3}mol L^{-1} min^{-1}) for the duplicate run with AIBN is much slower than that (2.3×10^{-2}mol L^{-1} min^{-1}) for the SPS counterpart. The value of R_p (= $[M]_0$ dX/dt, where $[M]_0$ is the initial monomer concentration (2.18 M in this series of experiments)) was obtained from the slope of the least-squares best-fitted straight line passing through the linear part of the X versus t data points (Fig. 5). Furthermore, the ultimate conversion (ca. 0.64) achieved for the duplicate run with AIBN is much lower than that (ca.0.85) for the SPS counterpart.

The dramatically different kinetic behaviors are primarily due to the quite different d versus X profiles for polymerizations initiated by AIBN and SPS, as shown in Fig. 6a. The value of d decreases rapidly from ca. 202 to 121 nm and then levels off with the progress of polymerization initiated by SPS, implying formation of tiny particle nuclei (ca. 10^0–10^1 nm in diameter) via other mechanisms such as homogeneous nucleation or micellar nucleation (if present; generally quite high levels of surfactants required to promote micellar nucleation due to the extremely large total miniemulsion droplet surface area) [38–41]. On the other hand, the extent of homogeneous nucleation is less for the duplicate run with AIBN (d decreases from ca. 222 to 161 nm and then levels off with the progress of polymerization) as compared to the SPS counterpart. It is interesting to note that even miniemulsion polymerizations initiated by AIBN show supporting evidence for the existence of homogeneous nucleation [26, 42, 43]. Generation of particle nuclei smaller than initial miniemulsion droplets results in a reduction in d. Nevertheless, the authors do not intend to go into details about particle nucleation and growth mechanisms because this subject is beyond the scope of this work. For those who are interested in this topic, refer to the aforementioned literature. In addition to polymerization of miniemulsion droplets, polymerization in monomer-swollen particle nuclei generated by homogeneous nucleation also contributes significantly to the overall rate of polymerization. The number density of initial miniemulsion droplets ($N_{d,i}$) was roughly estimated to be 4×10^{16} and 6×10^{16} L^{-1} for the duplicate run with AIBN and SPS, respectively, based on DLS data. In a similar manner, the number density of final latex particles ($N_{p,f}$) was roughly estimated to be 1×10^{17} and 3×10^{17} L^{-1} for the duplicate run with AIBN and SPS, respectively. Thus, the ratio of $N_{p,f}$ to $N_{d,i}$ ($N_{p,f}/N_{d,i}$) is equal to 2.5 and 5.0 for the duplicate run with AIBN and SPS, respectively. The higher the $N_{p,f}/N_{d,i}$, the stronger the homogeneous nucleation. These calculated

Table 1 Some representative R_O data for ST miniemulsions stabilized by PS costabilizers

Costabilizer	M_n	PDI	φ_p	$R_O \times 10^{21}$ (cm^3 s^{-1})	Ref.
PS_{lc}	8703	1.09	0.08	5.27	This work
PS_c	7142	1.68	0.08	16.98	[33]
PS_c	8967	1.84	0.08	18	[33]

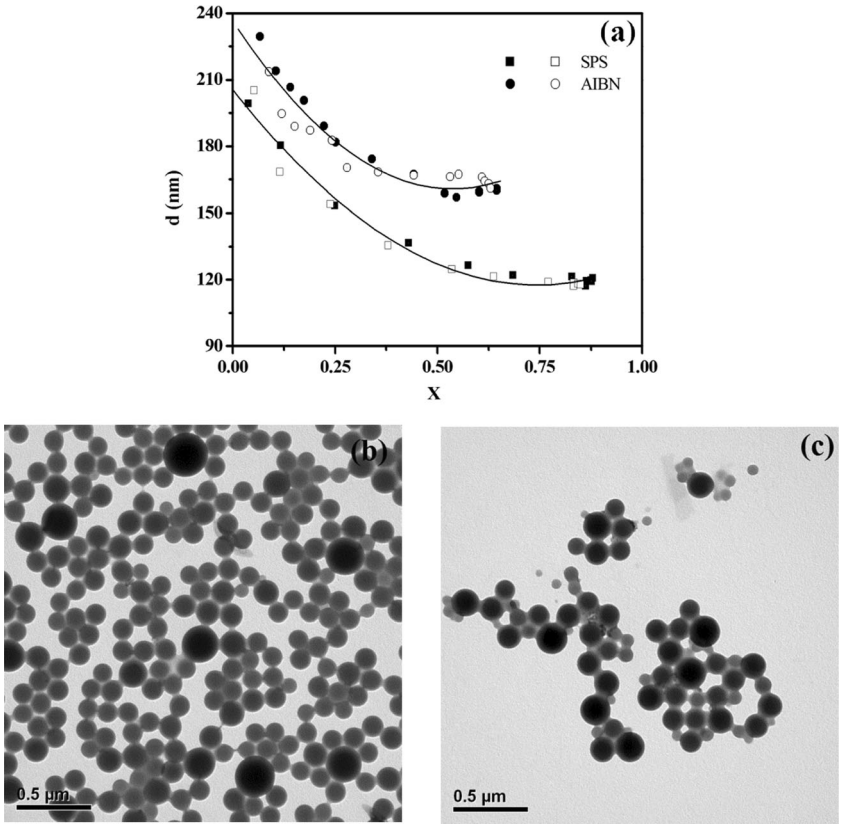

Fig. 6 **a** Hydrodynamic colloidal particle diameter of latex particles versus monomer conversion profiles for the miniemulsion polymerization of ST stabilized by PS_{lc} (φ_p=0.08) and initiated by 2.8 mM SPS based on total water volume or 15.0 mM AIBN based on the oil phase volume at 70 °C. (*filled square*, *white square*) SPS, (*filled circle*, *white circle*) AIBN. **b** and **c** TEM photographs for the final latex products with **b** SPS (at X=0.85) and **c** AIBN (at X=0.64) as the initiators

results further support the mixed mode of particle nucleation mechanisms for ST miniemulsion polymerization stabilized by PS_{lc} against Ostwald ripening and initiated by AIBN or SPS. It should be noted that R_p is linearly proportional to the number of latex particles per unit volume of water. The estimated $N_{p,f}$ data suggest that R_p for the SPS-initiated polymerization should be faster as compared to the AIBN-initiated polymerization. Furthermore, particle nuclei generated by homogeneous nucleation do not contain any PS_{lc} species since transport of these hydrophobic polymer costabilizer chains from miniemulsion droplets to particle nuclei originating from homogeneous nucleation is prohibited. As would be expected, polymerization in those particles in the absence of PS_{lc} (showing conventional emulsion polymerization characteristics) is much faster than that involved in PS_{lc}-stabilized miniemulsion droplets, in which RAFT polymerization is the predominant mechanism. Another minor factor is segregation of free radicals among polymerizing particles initiated by SPS that effectively suppresses the effect of bimolecular termination within particle nuclei originating from homogeneous nucleation. By contrast, thermal decomposition of AIBN generates two free radicals within a miniemulsion droplet, thereby leading to enhanced bimolecular termination of two neighboring radicals therein due to the cage effect. This then results in a reduction in the initiation efficiency involved in the AIBN-containing miniemulsion polymerization system. It is noteworthy that the initial rate of initiation ($R_i=2fk_d[I]_0$, where f is the initiator efficiency factor, k_d the initiation rate constant and $[I]_0$ the initial initiator concentration) is 1.13×10^{-3} and 4.66×10^{-5} mM s^{-1} for the runs with AIBN and SPS, respectively. In the calculation, f was arbitrarily taken as unity, k_d is equal to 3.78×10^{-5} and 2.33×10^{-5} s^{-1} at 70 °C for AIBN and SPS, respectively [44]. In general, R_p increases with increasing R_i. The reverse trend (R_p(SPS)>R_p(AIBN)) observed in this study simply implies that R_i does not play an important role in determining the polymerization kinetics. All these factors contribute to the dramatically different kinetic behaviors illustrated in Figs. 5 and 6a. Representative TEM photographs for the final latex products with SPS (at X=0.85) and AIBN (at X=0.64) as the initiators are shown in Fig. 6b and c, respectively. As expected, dry spherical polystyrene particles are observed. The weight-average particle diameter (d_w) and polydispersity index index (PDI defined as d_w/d_n, where d_n is the number-average particle diameter) are 107 nm and 1.02, respectively, for the run with SPS. As to the run with AIBN, the values of d_w and PDI are 140 nm and 1.22, respectively. Furthermore, DLS results are quite consistent with TEM observation; the values of d and polydispersity are 121 nm and 0.11, respectively, for the run with SPS, whereas they are 161 nm and 0.63, respectively, for the run with AIBN. Note that the larger the value of polydispersity, the broad the particle size distribution.

To gain a better understanding of the effect of initiators with different water solubilities (AIBN versus SPS) on polymerization kinetics, the following empirical equation [45–48] was used to simulate the kinetic data:

$$dX/dt = k(1-X)^m X^n \quad (2)$$

where k is the reaction rate constant and m and n are reaction orders. The modeling results are illustrated in Fig. 7 (MATLAB 2012A). The dX/dt versus X data were obtained from least-squares best-fitting the X versus t data in Fig. 5 with a polynomial of $X=a+bt+ct^2+dt^3$, followed by differentiating this polynomial with respect to t to give $dX/dt=b+2ct+3dt^2$. dX/dt was then expressed as a function of X with the aid of the polynomial $X=a+bt+ct^2+dt^3$. A general feature of RAFT miniemulsion polymerizations of ST stabilized by PS_{lc} and initiated by SPS or AIBN is that a maximal polymerization rate exists at X=ca. 0.40 and 0.25 for the duplicate run with SPS and AIBN, respectively. The kinetic parameters (k, m and n) at 70 °C thus obtained are (3.89×10^{-2} min^{-1}, 1.0610, 0.5316) and (1.85×10^{-2} min^{-1}, 1.9770, 0.6352) for the duplicate run with SPS and AIBN, respectively. The SPS-initiated RAFT miniemulsion polymerization shows a larger k, distinctly lower m and slightly lower n as compared to the AIBN counterpart. The quite different reaction orders of m provide supporting evidence for the quite different RAFT miniemulsion polymerization kinetics arising from original loci (continuous aqueous phase for SPS versus miniemulsion droplets for AIBN) for initiation reactions to take place.

Another important effect of homogeneous nucleation is the deviation from ideal evolution of molecular weight and molecular weight distribution of PS during RAFT miniemulsion polymerization (Figs. 8 and 9). The dashed line represents the least-squares best-fitted straight line passing through the experimental data points (i.e., the M_n versus X data) for the duplicate run with AIBN (or SPS). Thus, the coefficient of determination (R^2) of the least-squares best-fit result serves as an indicator for evaluating the quality of RAFT polymerization. That is, the higher the value of R^2, the better the control of polymer molecular weight growth. The value of R^2 is 0.9684 and 0.9812 for the duplicate run with AIBN and SPS, respectively. This result indicates that RAFT polymerization mechanism still predominates in the ST miniemulsion system regardless of the type of initiator used, even though conventional free radical polymerization within particle nuclei generated by homogeneous nucleation and other side reactions (e.g., bimolecular termination involved in the RAFT polymerization mechanism) within particles originating from miniemulsion droplets do occur therein.

The solid line in Fig. 8 represents the theoretical number-average molecular weight ($M_{n,th}=(n_{M,0}MW_M X/n_{RAFT,0})+MW_{RAFT}$, where $n_{M,0}$ and $n_{RAFT,0}$ are the initial number of moles of monomer and RAFT reagent and MW_M and MW_{RAFT} the molecular weight of monomer and RAFT reagent, respectively) as a function of X [49]. In this manner, the deviation of the M_n versus X data points from the $M_{n,th}$ versus X straight line, which is reflected in the coefficient of determination (R_{th}^2), serves as another useful indicator for studying RAFT miniemulsion polymerizations. Interestingly enough, deviation of the M_n versus X data from the theoretical solid line ($M_{n,th}$) for the duplicate run with AIBN (R_{th}^2= 0.1960) is slightly smaller than that (R_{th}^2=0.2033) for the SPS counterpart, that is, the experimental data for the duplicate run with SPS are closer to the theoretical solid line, as shown in Fig. 8. This result does not necessarily imply that ST miniemulsion polymerization initiated by SPS performs better in terms of polymer molecular weight control, as evidenced by the PDI versus X data shown in Fig. 9, and apparently oil-soluble AIBN is the initiator of choice in this study. One possible explanation for the M_n versus X data for the duplicate run with SPS is that a larger fraction of high molecular weight

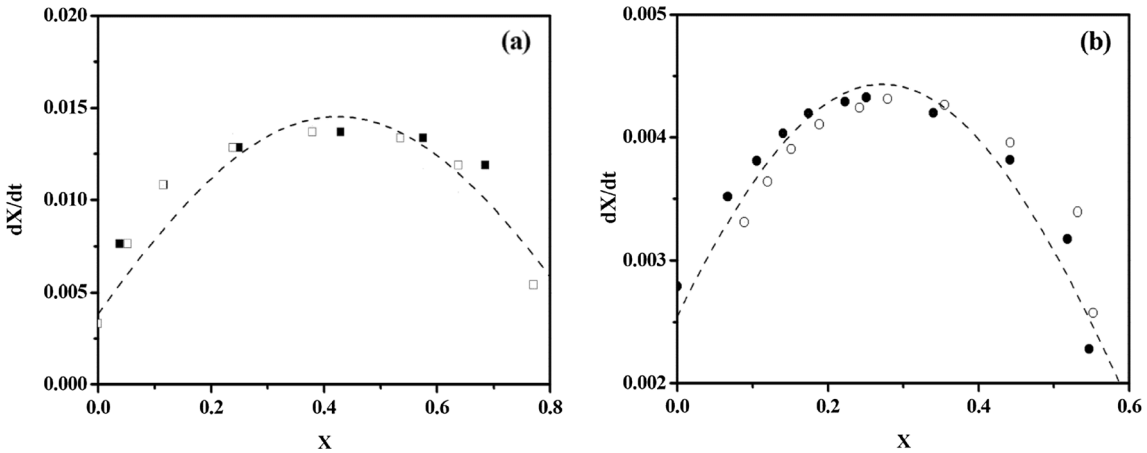

Fig. 7 dX/dt versus monomer conversion profiles for the miniemulsion polymerization of ST stabilized by PS_{lc} (φ_p=0.08) at 70 °C. **a** SPS and **b** AIBN. The *dashed line* represents the least-squares best-fitted result based on the empirical equation $dX/dt=k(1-X)^mX^n$

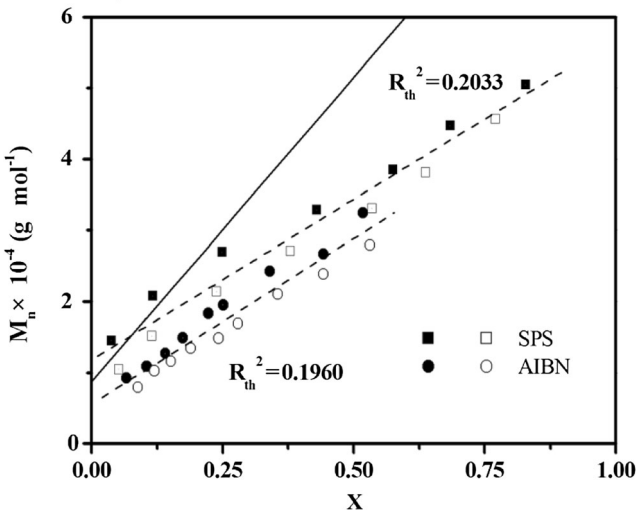

Fig. 8 Number-average molecular weight versus monomer conversion profiles for the miniemulsion polymerization of ST stabilized by PSlc (φp=0.08) and initiated by SPS or AIBN at 70 °C. (*filled square*, *white square*) SPS (R^2=0.9812), (*filled circle*, *white circle*) AIBN (0.9684). The solid line represents the theoretical number-average molecular weight ($M_{n,th}$). The dashed line represents the least-squares best-fitted straight line passing through the experimental data points for the duplicate run with AIBN (or SPS)

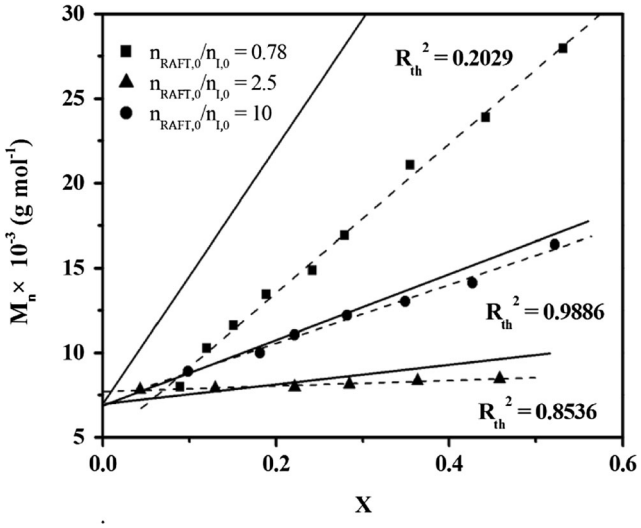

Fig. 10 Number-average molecular weight versus monomer conversion profiles for the miniemulsion polymerization of ST stabilized by PS_{lc} and initiated by AIBN at 70 °C. $n_{RAFT,0}/n_{I,0}$: (*filled square*) 0.78 (R^2=0.9976), (*filled triangle*) 2.5 (0.9954), (*filled circle*) 10 (0.9767). The solid line represents the theoretical number-average molecular ($M_{n,th}$). The *dashed line* represents the least-squares best-fitted straight line passing through the experimental data points

PS formed inside particle nuclei originating from homogeneous nucleation pushes experimental data points upward, thereby leading to a larger value of R_{th}^2.

The above kinetic data clearly demonstrate controlled growth of PS_{lc} via the RAFT polymerization mechanism in the two-component disperse phase system, though some side reactions interfered with living free radical polymerization to an appreciable extent. To further study the effectiveness of RAFT polymerization, a series of AIBN-initiated ST miniemulsion polymerizations with the ratio of $n_{RAFT,0}$ to $n_{I,0}$ ($n_{RAFT,0}/n_{I,0}$) being set at 0.78 ($n_{RAFT,0}$= 3.80×10^{-4} and $n_{I,0}$=4.87×10^{-4} mol), 2.50 ($n_{RAFT,0}$=1.22×10^{-3} and $n_{I,0}$=4.87×10^{-4} mol) and 10 ($n_{RAFT,0}$=2.44×10^{-3} and $n_{I,0}$=2.44×10^{-4} mol) were conducted, and the results summarized in Fig. 10 and 11. Note that the run with the highest $n_{RAFT,0}/n_{I,0}$ was achieved by using one half of $n_{I,0}$

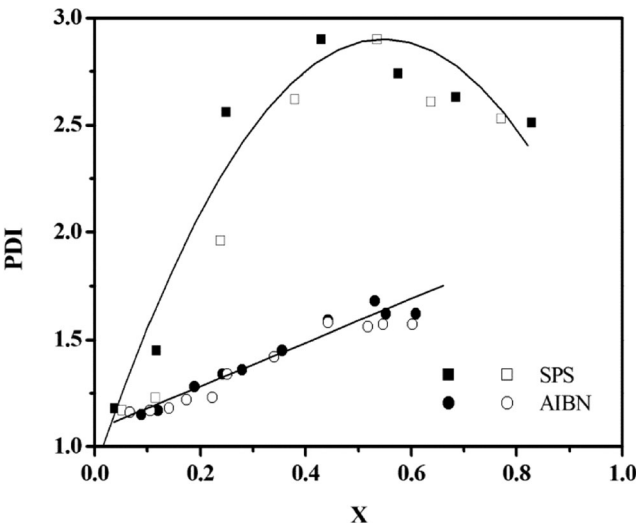

Fig. 9 Molecular weight distribution (PDI) versus monomer conversion profiles for the miniemulsion polymerization of ST stabilized by PS_{lc} (φ_p=0.08) and initiated by SPS or AIBN at 70 °C. (*filled square*, *white square*) SPS, (*filled circle*, *white circle*) AIBN

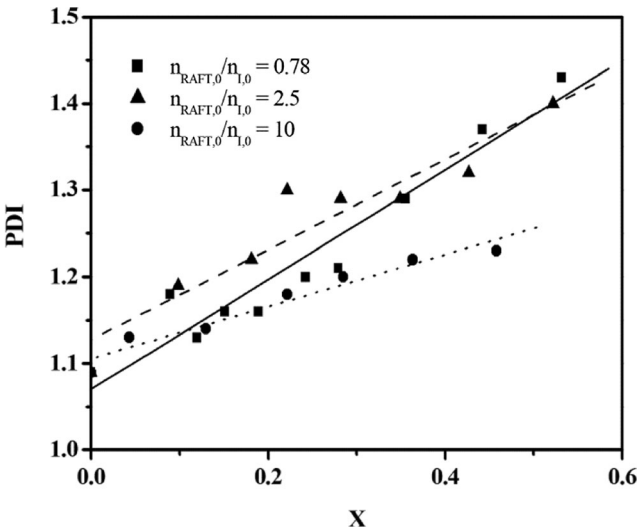

Fig. 11 Molecular weight distribution (PDI) versus monomer conversion profiles for the miniemulsion polymerization of ST stabilized by PS_{lc} and initiated by AIBN at 70 °C. $n_{RAFT,0}/n_{I,0}$: (*filled square*) 0.78 (0.9649), (*filled triangle*) 2.5 (0.9476), (*filled circle*) 10 (0.9767). The numeric value in the parenthesis represents the R^2 for the least-squares best-fitted straight line passing through the PDI versus X data points

and 6.41 times as much as $n_{RAFT,0}$ in the formulation with $n_{RAFT,0}/n_{I,0}=0.78$. In this manner, the viscosity of PS_{lc} solution was adequate to allow successful formation of ST miniemulsion. Figure 10 shows that the value of R^2 for the least-squares best-fitted discontinuous straight line passing the M_n versus X data for the run with $n_{RAFT,0}/n_{I,0}$ greater than 0.78 is larger than the duplicate run with $n_{RAFT,0}/n_{I,0}=0.78$. This implies that increasing $n_{RAFT,0}/n_{I,0}$ results in well controlled growth of PS_{lc} chains during RAFT miniemulsion polymerization. More importantly, deviation between the experimental data and theoretical evolution of molecular weight for PS_{lc} (see the solid lines in Fig. 10) is greatly reduced when $n_{RAFT,0}/n_{I,0}$ is greater than 0.78. Nevertheless, the greatly increased RAFT polymerization characteristics with $n_{RAFT,0}/n_{I,0}$ is achieved at the expense of desirable fast polymerization rate. The corresponding PDI versus X data are shown in Fig. 11. For comparison, least-squares best-fitted straight lines passing through the PDI versus X data points are included in the plot. It is shown that changes in PDI with X (i.e., the slope of the least-squares best-fitted straight line) in increasing order is: $n_{RAFT,0}/n_{I,0}=10$ (slope=0.30)$<n_{RAFT,0}/n_{I,0}=2.50$ (slope=0.52)$<n_{RAFT,0}/n_{I,0}=0.78$ (slope=0.63). This trend implies that the higher the $n_{RAFT,0}/n_{I,0}$, the stronger the effect of the RAFT polymerization mechanism on the RAFT miniemulsion polymerization of ST.

Conclusion

RAFT Miniemulsion polymerizations of ST with living polystyrene (PS_{lc}) serving as both RAFT reagent and polymer costabilizer were investigated. The miniemulsion upon aging at 25 °C showed satisfactory stability against the diffusional degradation of monomer droplets (Ostwald Ripening). The rate of polymerization for RAFT miniemulsion polymerization of ST initiated by oil-soluble AIBN at 70 °C is much slower than that for the water-soluble SPS counterpart. Furthermore, the ultimate conversion achieved for the run with AIBN is much lower than that for the SPS counterpart. In addition to the predominant monomer droplet nucleation, much stronger particle nucleation taking place in the continuous aqueous phase (homogeneous nucleation) for the run with AIBN was observed. It is the different extents of homogeneous nucleation that is responsible for the quite different kinetic behaviors between the RAFT miniemulsion polymerizations initiated by different types of initiator (AIBN versus SPS). To further study the effectiveness of RAFT polymerization, a series of AIBN-initiated ST miniemulsion polymerizations with different initial molar ratios of RAFT reagent to AIBN ($n_{RAFT,0}/n_{I,0}$) were carried out. Increasing $n_{RAFT,0}/n_{I,0}$ greatly promotes the influence of RAFT polymerization mechanism on evolution of polymer molecular weight and molecular weight distribution (i.e., better control over polymer chain growth), but at the expense of desirable fast polymerization rate generally experienced in conventional miniemulsion polymerization.

Acknowledgments Financial support from National Science Council, Taiwan is gratefully acknowledged.

References

1. Matyjaszewski K, Davis TP (2003) In: Handbook of Radical Polymerization. Wiley, Hoboken, Chapter 8, p 361
2. Matyjaszewski K, Spanswick J (2005) Mater Today 8:26
3. Coessens V, Pintauer T, Matyjaszewski K (2001) Prog Polym Sci 26:337
4. Nicolas J, Guillaneuf Y, Lefay C, Bertin D, Gigmes D, Charleux B (2013) Prog Polym Sci 38:63
5. Moad G, Rizzardo E, Thang SH (2008) Polymer 49:1079
6. Ganjeh-Anzabi P, Haddadi-Asl V, Salami-Kalajahi M, Abdollahi M (2013) J Polym Res 20:248
7. Ma J, Zhang H (2014) J Polym Res 21:614
8. Lansalot M, Farcet C, Charleux B, Vairon JP (1999) Macromolecules 32:7354
9. Moad G, Rizzardo E, Thang SH (2005) Aust J Chem 58:379
10. Barner L, Davis TP, Stenzel MH, Barner-Kowollik C (2007) Macromol Rapid Commun 28:539
11. Lowea AB, McCormick CL (2007) Prog Polym Sci 32:283
12. McLeary JB, Klumperman B (2006) Soft Matter 2:45
13. Qiu J, Charleux B, Matyjaszewski K (2001) Prog Polym Sci 26: 2083
14. Matyjaszewski K, Davis TP (2003) In: Handbook of Radical Polymerization. Wiley, Hoboken. Chapter 12, p 629
15. Chiefari J, Chong YK(B), Ercole F, Krstina J, Jeffery J, Le TPT, Mayadunne RTA, Meijs GF, Moad CL, Moad G, Rizzardo E, Thang SH (1998) Macromolecules 31:5559
16. Mayadunne RTA, Jeffery J, Moad G, Rizzardo E (2003) Macromolecules 36:1505
17. Mishra V, Kumar R (2012) J Sci Res 56:141
18. Antonietti M, Landfester K (2002) Prog Polym Sci 27:689
19. Butte A, Storti G, Morbidelli M (2000) Macromolecules 33:3485
20. Monteiro MJ, Barbeyrac JD (2001) Macromolecules 34:4416
21. Uzulina I, Kanagasabapathy S, Claverie J (2000) Macromol Symp 150:33
22. Monteiro MJ, Hodgson M, Brouwer HD (2000) J Polym Sci Polym Chem 38:3864
23. Moad G, Chiefari J, Chong YK(B), Krstina J, Mayadunne RTA, Postma A, Rizzardo E, Thang SH (2000) Polym Int 49:993
24. Chern CS (2008) In: Miniemulsion Polymerization. Principles and Applications of Emulsion Polymerization. Wiley, Hoboken. p 128
25. Asua JM (2002) Prog Polym Sci 27:1283
26. Chern CS, Liou YC (1999) J Polym Sci Pol Chem 37:2537
27. Lin M, Hsu JCC, Cunningham MF (2006) J Polym Sci Pol Chem 44:5974
28. Chern CS, Chang HT (2002) Polym Int 51:1428
29. Remiers JL, Schork FJ (1996) J Appl Polym Sci 59:1833
30. Remiers JL, Schork FJ (1996) J Appl Polym Sci 60:251
31. Senyek ML, Kulig JJ, Paker DK, The Goodyer Tire and Rubber Co (2002) US Pstent 6(369):158
32. Vale H, Mckenna T (2005) Colloid Surf A-Physicochem Eng Asp 268:68
33. Chen LJ, Lin SY, Chern CS, Wu SC (1997) Colloid Surf A-Physicochem Eng Asp 122:161
34. Morton M (1954) J Colloid Interface Sci 9:300

35. Lin CT, Wu JM, Chern CS (2013) Colloid Surf A-Physicochem Eng Asp 434:178
36. Lifshitz IM, Slozov VV (1958) Zh Exp Thor Fiz (in Russian) 35: 479
37. Kabalnov AS, Pertzov AV, Shchukin ED (1987) Colloid and Surf 24:19
38. Chern CS, Liou YC, Chen TJ (1998) Macromol Chem Phys 199: 1315
39. Chern CS, Chen TJ, Liou YC (1998) Polymer 39:3767
40. Chern CS, Liou YC (1998) Macromol Chem Phys 199:2051
41. Chang HC, Lin YY, Chern CS, Lin SY (1998) Langmuir 14:6632
42. Alduncin JA, Forcada JF, Barandiaran MJ, Asua J (1991) J Polym Sci Part A Polym Chem 29:1265
43. Nomura M, Ikoma J, Fujita K (1993) J Polym Sci Part A: Polym Chem 31:2103
44. Bandrup J, Inmergut EH, Grulke EA (1998) Polymer handbook, 4th edn. Wiley, Hoboken
45. Sestak J, Berggern G (1971) Thermochim Acta 3:1
46. Vyazovkin S, Burmham AK, Criado JM, Perez-Maqueda LA, Popescu C, Sbirrazzuoli N (2011) Thermochim Acta 520:1
47. Khawam A, Fanagan DR (2006) J Phys Chem B 110:17315
48. Vyazovkin S, Sbirrazzuoli N (2006) Macromol Rapid Commun 27: 1515
49. Tsavalas JG, Schork FJ, Brouwer H d, Monteiro MJ (2001) Macromolecules 34:3938